

Relation between the Vibration Frequencies of a Crystal and the Scattering of Slow Neutrons

G. L. SQUIRES*

Institute for Advanced Study, Princeton, New Jersey

(Received April 6, 1956)

Detailed calculations of the scattering of slow neutrons by crystals have so far been made on the basis of the Debye approximation for the vibration frequencies of the crystal. In the present work, a somewhat more realistic set of frequencies has been calculated for the case of aluminum. The results have been used to calculate the angular and energy distribution of neutrons coherently scattered in a one-phonon process. Comparison is made with the results given by the Debye approximation.

The distribution function of the calculated frequencies has been used to obtain values for the Debye-Waller factor and for the total incoherent cross section for incident neutrons with long wavelengths.

I. INTRODUCTION

THE scattering of slow neutrons by crystals has been the subject of much theoretical and experimental study in recent years. In order to calculate the scattering theoretically, it is necessary to know the relation between the frequency ν , wave vector \mathbf{q} , and polarization l for the normal vibrations of the crystal. Quantitative estimates of the scattering have been made by several authors¹ on the basis of the Debye assumption, *viz.*, that the velocity of the vibrations is a constant, independent of the wavelength, polarization, and direction of propagation.

The question of the influence of the function $\nu_l(\mathbf{q})$ on neutron scattering has been discussed by Placzek and Van Hove.² They point out that the Debye approximation is not reliable for predicting the angular and energy distribution of the scattered neutrons, because the distribution depends sensitively on the details of the function $\nu_l(\mathbf{q})$. On the other hand, for such quantities as the Debye-Waller factor in the Bragg reflection of neutrons and also for the total incoherent cross sections, calculations based on the Debye approximation may be quite good. This is because both of these quantities involve the average properties of the function $\nu_l(\mathbf{q})$, *i.e.*, they involve certain functions of the frequency averaged over all the frequencies; and it is known from the theory of the specific heats of solids, which likewise involves the average properties of the function $\nu_l(\mathbf{q})$, that the Debye theory gives fairly good results in such cases.

In the present paper, we use a somewhat more realistic set of frequencies than that of Debye in order to calculate the scattering of neutrons by a crystal of aluminum. The frequencies were obtained from a simple model of the interatomic forces in the crystal. The forces were chosen to give the best fit to the experimentally determined values of the elastic constants and also to the results of Walker³ who, by means of

x-ray measurements on aluminum, has measured some of the frequencies.

The calculations fall into two parts. In the first part, Secs. II and III, we calculate the angular and energy distribution of neutrons scattered coherently in the process in which they exchange energy with the crystal by exciting or de-exciting one phonon in the lattice. It is this process which depends most directly on the details of the function $\nu_l(\mathbf{q})$. The results obtained from the Debye approximation are given for comparison. In the second part, Sec. IV, we calculate the Debye-Waller factor, and the total incoherent cross section in the limiting case of very slow incident neutrons, where the cross section varies linearly with neutron wavelength.

II. CALCULATION OF THE VIBRATION FREQUENCIES

A. General Properties of the Normal Vibrations

The properties of the normal vibrations have been discussed by several authors.⁴ We here summarize those relevant to our calculations.

Consider a crystal containing N atoms arranged in a Bravais lattice. Let $\boldsymbol{\tau}$ be a lattice vector in the reciprocal lattice.

On the assumption that the interatomic forces are harmonic, the displacements of the lattice points in the crystal may be treated as the sum of the displacements of a set of plane sinusoidal waves, known as the normal vibrations. We define the wave vector \mathbf{q} of a normal vibration so that its magnitude is equal to the reciprocal of the wavelength. Corresponding to each \mathbf{q} there are three independent waves with polarizations specified by $l=1, 2, 3$ and frequencies $\nu_l(\mathbf{q})$.

The normal waves are only defined by their displacements at the lattice points. Therefore, since the waves \mathbf{q} and $\mathbf{q}+\boldsymbol{\tau}$ give the same displacements at the lattice points, they represent the same physical waves, and $\nu_l(\mathbf{q})$ must satisfy the relation

$$\nu_l(\mathbf{q}) = \nu_l(\mathbf{q} + \boldsymbol{\tau}).$$

* Now at the Cavendish Laboratory, Cambridge, England.

¹ For references, see G. Placzek and L. Van Hove, *Phys.* **93**, 1207 (1954).

² G. Placzek and L. Van Hove, *Nuovo cimento* **1**, 233 (1955).

³ C. Walker (private communication).

⁴ L. Brillouin, *Wave Propagation in Periodic Structures* (Dover Publications, Inc., New York, 1953), and M. Born and K. Huang, *Dynamical Theory of Crystal Lattices* (Oxford University Press, London, 1954).

It is thus sufficient to confine our attention to those \mathbf{q} that lie in a single cell in the reciprocal lattice. The cell usually taken is the first Brillouin zone surrounding the origin.

The values of \mathbf{q} are further restricted by imposing the condition that the wavelengths of the normal waves along the directions of the unit cell vectors in the crystal must be exact submultiples of the dimensions of the crystal in those directions. The \mathbf{q} points so restricted form a lattice with N points in each zone of reciprocal space. Since each \mathbf{q} point represents three vibrations, we have $3N$ normal vibrations, which is the correct number to describe the displacements of the N particles in the crystal lattice.

In practice, N is very large and the \mathbf{q} points are therefore very close to each other. In the calculation of the function $\nu_l(\mathbf{q})$, no difficulty arises if \mathbf{q} is assumed to be defined at all points in reciprocal space.

B. Force Model

The lattice of aluminum is face-centered cubic and its reciprocal lattice is therefore body-centered cubic (Fig. 1). Denote the length of the cube side in the reciprocal lattice by $2b=2/a$, where a is the length of the cube side in the crystal lattice. Take orthogonal axes q_1, q_2, q_3 in reciprocal space. (In Fig. 1 and throughout the paper, coordinates of points in reciprocal space are given in units of b .)

We assume that the crystal forces are harmonic and that they exist only between first and second nearest neighbors.⁵ On these assumptions, it may be shown⁶ that the most general set of forces is specified by five force constants: three for the first nearest, and two for the second nearest neighbor forces.

The equation giving ν as a function of \mathbf{q} is

$$|T(\mathbf{q}) - \mu^2 I| = 0. \quad (1)$$

The left-hand side is a 3×3 determinant whose ele-

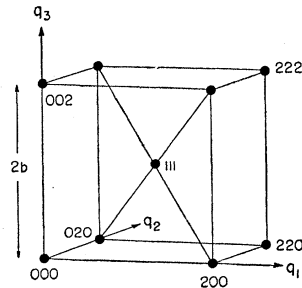


FIG. 1. Reciprocal lattice of aluminum.

⁵ Owing to the presence of the conduction electrons in a metal, the extent to which the present simple model is valid for aluminum may be questioned. However, at the moment there does not appear to be a satisfactory theory of lattice vibrations that takes the effects of these electrons into account, and the present model is used for want of a better one.

⁶ M. Born and G. H. Begbie, Proc. Roy. Soc. (London) **A188**, 179 (1947).

TABLE I. Numerical values of constants used in the calculation of $F(\mathbf{q})$.

| Elastic constants (10^{12} dynes/cm ²) | Force constants (10^3 dynes/cm) |
|--|---------------------------------------|
| $c_{11}=1.092$ | $\alpha_1=-1.3$ |
| $c_{12}=0.640$ | $\beta_1=7.7$ |
| $c_{44}=0.284$ | $\gamma_1=9.3$ |
| | $\alpha_2=3.3$ |
| | $\beta_2=-0.3$ |

ments are given by

$$T_{ii} = \alpha_1 + 2\beta_1 - \alpha_1 C_j C_k - \beta_1 C_i (C_j + C_k) + \alpha_2 S_i^2 + \beta_2 (S_j^2 + S_k^2),$$

$$T_{ij} = \gamma_1 S_i S_j \quad (i \neq j),$$

$$\mu^2 = M \pi^2 \nu^2,$$

$$C_i = \cos \theta_i, \quad S_i = \sin \theta_i, \quad \theta_i = \pi q_i / b.$$

I is the unit matrix. M is the mass of an aluminum nucleus. $\alpha_1, \beta_1, \gamma_1$ are the force constants for the first nearest and α_2, β_2 the force constants for the second nearest neighbor interactions.

For each value of \mathbf{q} , Eq. (1) has three solutions, $\nu_l (l=1,2,3)$. In order to relate the solutions at different \mathbf{q} points, we follow the suggestion of Rosenstock⁷ and define the three frequency branches so that the waves with the highest of the three frequencies at each \mathbf{q} point constitute one branch; those with the middle frequency, another; and those with the lowest frequency, the third.

The relations between the force constants $\alpha_1, \beta_1, \gamma_1, \alpha_2, \beta_2$ and the elastic constants c_{11}, c_{12}, c_{44} are found by allowing $|\mathbf{q}|$ to tend to zero in Eq. (1) and comparing the limiting equation with the equation relating frequency and wave vector for acoustical waves.⁸ The relations are

$$\begin{aligned} \beta_1 + \alpha_2 &= \frac{1}{4} a c_{11}, \\ \alpha_1 + \beta_1 + 2\beta_2 &= \frac{1}{2} a c_{44}, \\ \gamma_1 &= \frac{1}{4} a (c_{44} + c_{12}). \end{aligned} \quad (2)$$

The numerical values adopted for the elastic constants are given in Table I. They represent the average of the values obtained at room temperature (293°K) by Lazarus,⁹ Long and Smith,¹⁰ and Sutton.¹¹

In order to obtain values for the five force constants, further data are needed. These were provided by the results of Walker,³ who has measured the intensities of x-rays scattered from a single crystal of aluminum. By means of these measurements, it is possible to calculate the frequencies of those vibrations with wave vectors lying along the edges, and the body and face diagonals of the reciprocal cube. The values of the

⁷ H. B. Rosenstock, Phys. Rev. **97**, 290 (1955).

⁸ J. de Launay, J. Chem. Phys. **21**, 1975 (1953).

⁹ D. Lazarus, Phys. Rev. **76**, 545 (1949).

¹⁰ T. R. Long and C. S. Smith, Office of Naval Research Technical Report No. 12, 1953 (unpublished).

¹¹ P. M. Sutton, Phys. Rev. **91**, 816 (1953).

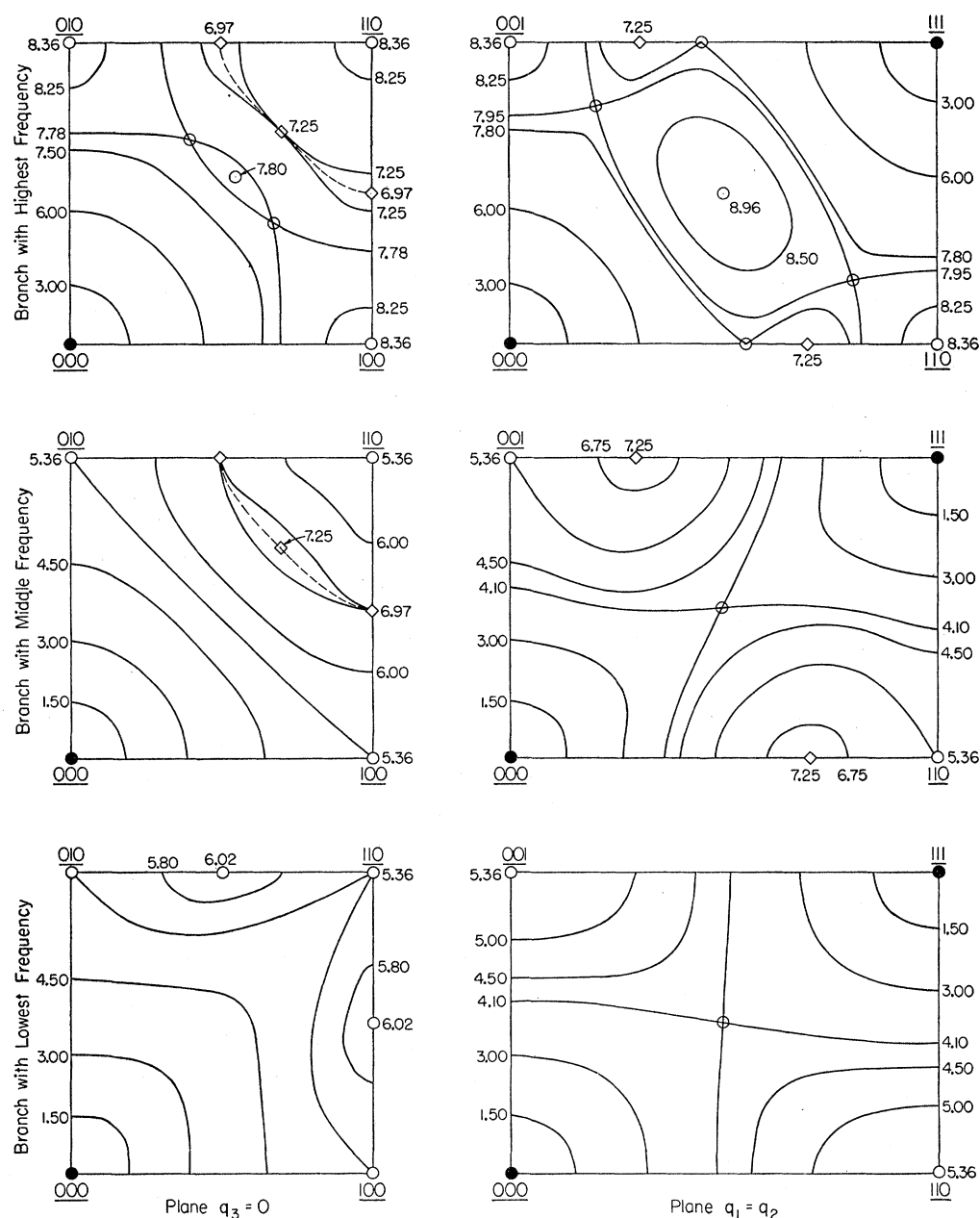


FIG. 2. Curves of constant frequency in the planes $q_3=0$ and $q_1=q_2$ for the three branches. The numbers beside the curves and points indicate the value of the frequency in units of 10^{12} sec^{-1} . The numbers underlined are the coordinates of the corner points. --- locus of points along which the two upper frequencies are equal; ● reciprocal lattice point; ○ critical point; ◇ generalized critical point. (The critical points are discussed in Sec. IV. B.)

force constants given in Table I are those which, subject to the condition that they satisfy the values adopted for the elastic constants, give the best fit to the frequencies obtained from the x-ray measurements.

In order to obtain these frequencies, the measured values of the x-ray intensities must be corrected for the effects of Compton and multiphonon scattering. The final values of the frequencies are subject to error from the uncertainty of these corrections. The rms difference between the values of the frequencies, calculated from Eq. (1) with the values of the force constants given in Table I, and the experimental values is about 4 percent. This is of the same order as the error in the latter. The

resulting uncertainty in the force constants is about $\frac{1}{2}$ to 1 in units of 10^8 dynes/cm .

C. Computation of the Frequencies

The particular $\nu_l(\mathbf{q})$ function obtained when the numerical values of the force constants in Table I are inserted in Eq. (1) is denoted by $F(\mathbf{q})$. This function was computed for all points whose coordinates q_i were integral multiples of $b/10$. The number of such points which are different, i.e., not converted into each other by the operations of symmetry, is 152. The calculations of the frequency were carried out on the electronic computer at the Institute for Advanced Study.

Some of the results are shown in Fig. 2, where curves of constant frequency in the planes $q_3=0$ and $q_1=q_2$ are shown for the three branches.

III. COHERENT ONE-PHONON SCATTERING

A. Scattering Surface

Let a beam of monoenergetic neutrons be incident on a single crystal and consider a neutron coherently scattered by a process in which it exchanges one phonon with an oscillator of wave vector \mathbf{q} and frequency $\nu_l(\mathbf{q})$. Let \mathbf{k}_0 and \mathbf{k} be the initial and final wave vectors of the neutron. Put $\boldsymbol{\kappa} = \mathbf{k} - \mathbf{k}_0$.

The interference of the scattered waves gives the condition

$$\mathbf{k} - \mathbf{k}_0 = \mathbf{q} + \boldsymbol{\tau}. \quad (3)$$

Conservation of energy gives

$$k^2 - k_0^2 = \pm \frac{2m}{h} \nu_l(\mathbf{q}), \quad (4)$$

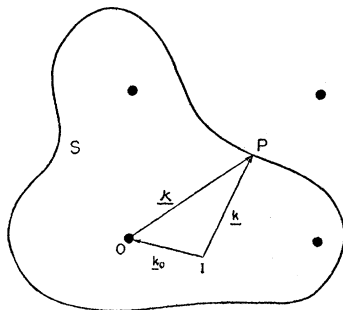
where m is the mass of the neutron. The sign on the right-hand side of Eq. (4) is positive if the neutron absorbs and negative if it emits a phonon.

If \mathbf{k}_0 is fixed relative to the crystal, only certain values of \mathbf{k} , viz, those that can satisfy Eqs. (3) and (4) for some value of \mathbf{q} , are possible. Let O be the origin in reciprocal space (Fig. 3), and let IO represent the vector \mathbf{k}_0 . P is a point such that IP represents a possible \mathbf{k} , i.e., one that satisfies Eqs. (3) and (4). The locus of all such points is a surface, termed a scattering surface S .

The concept of the scattering surface has been discussed by Lowde¹² and Placzek and Van Hove.¹ For given \mathbf{k}_0 , the surface depends only on the relation between ν_l and \mathbf{q} . Since there are three such relations, one corresponding to each frequency branch, S consists in general of three surfaces.

The present calculations of the coherent one-phonon scattering have been carried out in terms of the scattering surface. The majority of the calculations have been carried out for the case $k_0=0$, i.e., for incident neutrons of infinite wavelength. These calculations indicate the essential features of the surfaces. In addition, sections of

FIG. 3. Scattering surface.



¹² R. D. Lowde, Proc. Roy. Soc. (London) A221, 206 (1954).

FIG. 4. Section through the scattering surface S_F at the plane $q_3=0$. ($k_0=0$). The surfaces corresponding to the two lower frequencies are usually very close together. To help distinguish them in Figs. 4, 6, 9, and 10, the section corresponding to the lowest frequency is shown as a broken curve.

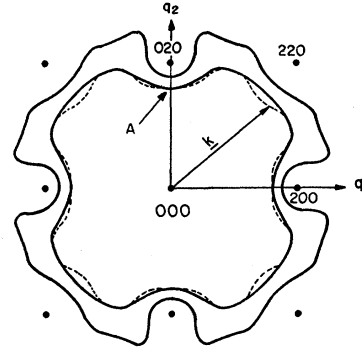
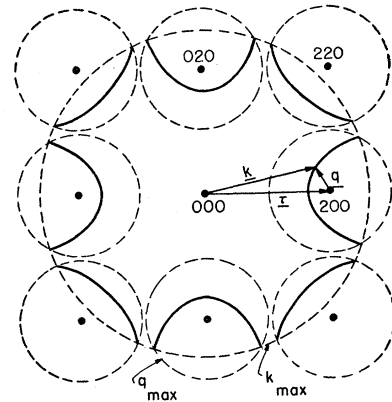


FIG. 5. Section through the Debye scattering surface at the plane $q_3=0$ ($k_0=0$).



the surfaces have been calculated for two other values of k_0 .

B. Incident Neutrons of Infinite Wavelength

In this case, the scattering surfaces have the same symmetry as the reciprocal lattice. The only process to be considered is one in which the neutron absorbs a phonon from the thermal vibrations of the crystal.

Figures 4 and 5 show sections through the scattering surfaces at the plane $q_3=0$. Figure 4 shows the section given by the function $F(\mathbf{q})$. (The scattering surfaces obtained from $F(\mathbf{q})$ are denoted by S_F .) Figure 5 shows the section of the surface obtained on the basis of the Debye approximation $\nu = c|\mathbf{q}|$, with the constant c taken to have the value 3.40×10^5 cm/sec. This corresponds to a Debye temperature $\Theta = 398^\circ\text{K}$, the value obtained from specific heat measurements.¹³

There are two features to be noted in comparing the scattering curves:

1. In the Debye case, it is possible to identify each part of the scattering surface with a particular reciprocal lattice vector $\boldsymbol{\tau}$. The parts corresponding to different $\boldsymbol{\tau}$'s do not join continuously. This is because, in the Debye approximation, ν is not a continuous function of \mathbf{q} , defined at all points in \mathbf{q} space.

On the other hand, in the correct theory, whatever the actual $\nu_l(\mathbf{q})$ function may be, it must be both

¹³ G. Borelius, *Handbuch der Metallphysik* (Akademische Verlagsgesellschaft, 1935), Vol. 1, Part 1, p. 252.

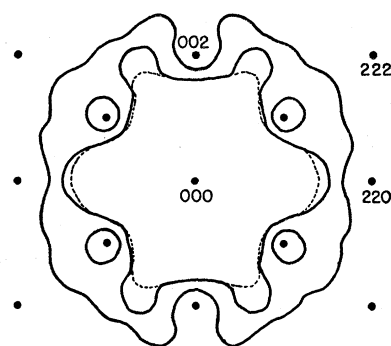


FIG. 6. Section through the scattering surface S_F at the plane $q_1 = q_2$ ($k_0 = 0$).

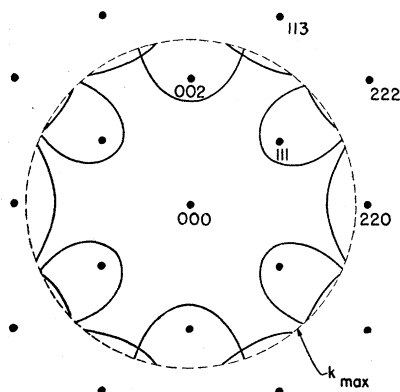


FIG. 7. Section through the Debye scattering surface at the plane $q_1 = q_2$ ($k_0 = 0$).

continuous and everywhere defined. Consequently, the scattering surface must also be continuous as shown in Fig. 4. Unless a scattering surface lies wholly within one Brillouin zone (an example of this occurs in Fig. 6), there is no physical meaning to the identification of any part of the surface with a particular reciprocal lattice point. When the surface passes from one zone to another, it does so smoothly.

2. In the Debye case (Fig. 5), it is possible to draw a straight line from the origin in such a direction that it does not cut the scattering curve. The physical meaning of this is that no neutrons are scattered along that direction. The existence of such directions contradicts a general theorem of Placzek and Van Hove¹ that neutrons are scattered in every direction. The reason for the contradiction is again the fact that the Debye frequency function does not possess the properties of being continuous and everywhere defined in \mathbf{q} space.

In Fig. 4, the scattering curves for two of the frequency branches are seen to coincide along the q_1 and q_2 axes. This is because two of the waves have equal frequencies along these directions, a result which is generally true for cubic lattices and does not depend on a particular force model.

It must be remembered that the scattering surfaces indicate only the momenta of the neutrons scattered in different directions. The intensities of the scattered neutrons are given by the cross-section formulas. The cross section for the coherent one-phonon process

contains a factor $[\mathbf{k} \cdot \mathbf{e}_l(\mathbf{q})]^2$, where $\mathbf{e}_l(\mathbf{q})$ is the unit polarization vector. The two waves with equal frequencies along the q_1 and q_2 axes are pure transverse waves. Thus in their case the factor is zero, and no neutrons corresponding to the point A in Fig. 4 would be observed.

Figures 6 and 7 show the sections of the scattering surfaces at the plane $q_1 = q_2$. The sections in Fig. 6 correspond to the function $F(\mathbf{q})$, and those in Fig. 7 correspond to the Debye frequency relation with $\Theta = 398^\circ\text{K}$. The features are similar to those exhibited in the plane $q_3 = 0$. The appearance in Fig. 6 of closed curves, which are sections of surfaces entirely within the zones surrounding the 111 points, may be noted. They correspond to the branch with the highest frequency.

In addition to the sections shown in Figs. 4 and 6, sections of the surface S_F have been calculated for the planes $q_3 = nb/10$, where n takes integral values from 1 to 26. Because of the labor involved, the work was confined to the surface corresponding to the highest frequency branch. The range of n was chosen to cover the whole surface. Sections for the values $n = 0, 5, 10, 15, 20$, and 25 are shown in Fig. 8.

C. Incident Neutrons of Finite Wavelength

To illustrate the case when the wavelength λ_0 of the incident neutrons is finite, the sections of the scattering surface S_F in the plane $q_3 = 0$ were calculated for $\lambda_0 = 6.74 \text{ \AA}$ ($k_0/b = 0.60$) and $\lambda_0 = 1.06 \text{ \AA}$ ($k_0/b = 3.81$), with \mathbf{k}_0 lying along the q_1 axis in both cases.

The value $\lambda_0 = 6.74 \text{ \AA}$ was chosen as it lies in the wavelength region of neutrons obtained from filtered sources and slow choppers. The section through S_F is shown in Fig. 9.

The section through S_F for $\lambda_0 = 1.06 \text{ \AA}$ is shown in Fig. 10. This value of λ_0 is typical of those employed in crystal spectrometers. The initial energy of the neutrons is sufficient for the neutron to give energy to the crystal lattice (phonon emission). There are thus six surfaces

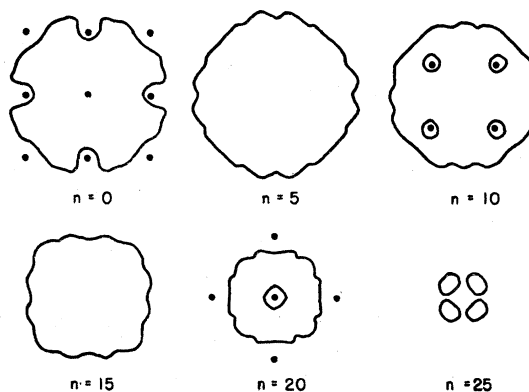


FIG. 8. Section through the scattering surface S_F for the highest frequency branch at the planes $q_3 = nb/10$ ($k_0 = 0$). \bullet reciprocal lattice point.

in all, three for phonon absorption and three for phonon emission.

There are two points to be noted in connection with Fig. 10:

1. The point $\tau=0$ is always a point on the scattering surface. (It corresponds to the undisturbed incident beam.) However, whether it is an isolated point or whether the scattering surface exists in the neighborhood of the origin depends on whether the velocity of the incident neutrons is less or greater than the maximum sound velocity, i.e., the maximum value of $v/|q|$ as q tends to zero from any direction. In the present case, the velocity of the incident neutrons lies between the maximum sound velocities of the highest and middle frequency branches. Thus, as Fig. 10 indicates, the scattering surfaces of the lower two frequencies emerge from the origin. That of the highest frequency does not.

2. If ν_{\max} is the maximum frequency that occurs, the maximum and minimum values that k can have are

$$k_{\max} = [k_0^2 + (2m/h)\nu_{\max}]^{\frac{1}{2}}$$

and

$$k_{\min} = [k_0^2 - (2m/h)\nu_{\max}]^{\frac{1}{2}}.$$

The scattering surfaces for phonon absorption must lie between the spheres of radius k_0 and k_{\max} , while those for phonon emission must lie between the spheres of radius k_{\min} and k_0 .

As k_0 becomes large, $k_{\max} - k_0$ and $k_0 - k_{\min}$ become small compared with k_0 . Thus the scattering surfaces tend to become spherical, a tendency that can be seen by comparing Figs. 9 and 10. The limiting case of spherical scattering surfaces is the one that applies to the scattering of x-rays, where it is always true that

$$|k_{\max, \min} - k_0| \ll k_0.$$

D. Discussion

Reports have been published of two experiments designed to measure the scattering surfaces of aluminum

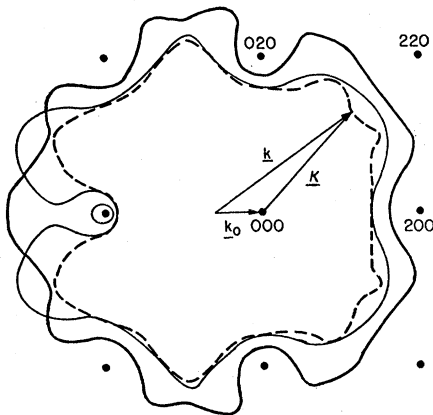


FIG. 9. Section through the scattering surface S_F at the plane $q_3=0$ for neutrons with $\lambda_0=6.74$ Å (k_0 along q_1 axis).

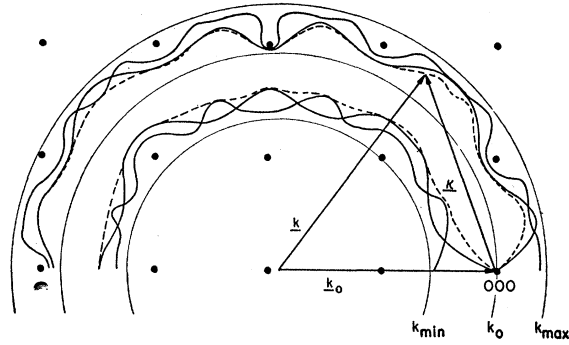


FIG. 10. Section through the scattering surface S_F at the plane $q_3=0$ for neutrons with $\lambda_0=1.06$ Å (k_0 along q_1 axis).

and hence to determine the crystal frequencies. Brockhouse and Stewart¹⁴ have made some measurements using two crystal spectrometers, one to produce a monoenergetic incident beam and the other to analyze the scattered neutrons. Carter *et al.*¹⁵ use neutrons filtered through beryllium for their incident beam and analyze the scattered neutrons with a slow chopper.

Both experiments have so far been of a preliminary nature, and the resolution has not been sufficient to locate the scattering surfaces with precision. However, as the intensities of neutron sources improve, such experiments will give increasing information on the function $\nu_i(q)$ and hence shed some light on the interatomic forces in crystals.

It has already been pointed out that underlying our calculation of the frequencies and the subsequent discussion of the scattering surfaces is the assumption of harmonic forces. On this assumption, the theory gives, for each q , three exact values of ν_i which are independent of the temperature of the crystal. The scattering surfaces that result are thus infinitely thin and independent of the temperature.

However, there are several phenomena, e.g., thermal expansion, which show that the interatomic forces in a crystal are not harmonic. If the anharmonic forces are small compared with the harmonic forces, they may be treated as a perturbation of the latter, and, to a first approximation, their effect is to cause each ν_i to spread over a small range of values. Both the range and the mean value of ν_i are functions of the temperature.

In calculating the function $F(q)$, we used room temperature (293°K) values of the elastic constants and the results of Walker's measurements which were also carried out at room temperature. We therefore calculated the set of frequencies that are the best fit to certain room temperature observations. They would not be the best fit to similar observations made at other temperatures.

Anharmonicity of the forces will therefore have two

¹⁴ B. N. Brockhouse and A. T. Stewart, Phys. Rev. **100**, 756 (1955).

¹⁵ Carter, Meuthner, Hughes, and Palevsky, Bull. Am. Phys. Soc. Ser. II, **1**, 55 (1956).

effects on the scattering surfaces. First, they will have a blurring effect on them, i.e., they will give them a finite thickness. Secondly, if we take the calculated surfaces as representing the mean positions of the scattering volumes, the surfaces will be subject to an increasing error as the temperature of the crystal departs from 293°K.

IV. FREQUENCY DISTRIBUTION FUNCTION AND NEUTRON SCATTERING

A. Introduction

It is of interest to consider the predictions by the function $F(\mathbf{q})$ for those aspects of neutron scattering which involve the average rather than the detailed properties of the function. For this purpose we have selected the Debye-Waller factor in the coherent elastic cross section and the total incoherent cross section for incident neutrons of long wavelength.

The differential coherent elastic cross section $d\sigma_{c,el}/d\Omega$ is given by¹⁶

$$\frac{d\sigma_{c,el}}{d\Omega} = \bar{a}^2 \exp(-4\pi^2\kappa^2\alpha_\kappa) \frac{1}{v_0} \sum_{\boldsymbol{\tau}} \delta(\boldsymbol{\kappa} + \boldsymbol{\tau}), \quad (5)$$

where v_0 is the volume per nucleus and \bar{a} is the scattering length averaged over all the nuclei in the crystal. In the sum over $\boldsymbol{\tau}$, the term $\boldsymbol{\tau}=0$ is excluded.

The factor $\exp(-4\pi^2\kappa^2\alpha_\kappa)$ is the Debye-Waller factor. The quantity α_κ is the average square of the displacement of a nucleus in the direction of $\boldsymbol{\kappa}$, the average being taken over the thermal equilibrium distribution. For a cubic crystal, α_κ is independent of the direction of $\boldsymbol{\kappa}$ and is given by

$$\alpha(T) = \frac{h}{8\pi^2 M} \frac{1}{3N} \sum_{\mathbf{q},l} A(\nu, T), \quad (6)$$

where

$$A(\nu, T) = \frac{1}{\nu} \coth \frac{h\nu}{2k_B T}.$$

M is the mass of the scattering nucleus, T is the temperature of the crystal, and k_B is Boltzmann's constant.

Placzek¹⁷ showed that the total incoherent cross section σ_i can be expanded in powers of m/M , the ratio of the mass of the neutron to the mass of the nucleus.

$$\sigma_i = s + \sum_{n=1}^{\infty} \sigma^{(n)} \left(\frac{m}{M} \right)^n, \quad (7)$$

where s is the bound incoherent cross section. For aluminum, $m/M=0.037$, and the series converges rapidly. We shall consider only the term $n=1$ in the

sum. As the wave number k_0 of the incident neutrons becomes small, $k_0\sigma^{(1)}$ tends to a finite limit $\beta(T)$, given by¹⁸

$$\beta(T) = s \left(\frac{2m}{h} \right)^{\frac{1}{2}} \frac{1}{3N} \sum_{\mathbf{q},l} B(\nu, T), \quad (8)$$

where

$$B(\nu, T) = \frac{\nu^{\frac{1}{2}}}{\exp(h\nu/k_B T) - 1}.$$

We therefore see that the evaluation of both the Debye-Waller factor for elastic scattering and the total incoherent cross section at long wavelengths depends on the value of some function $C(\nu, T)$ ($C=A$ or B) averaged over the $3N$ values of the frequency given by the N points in the first Brillouin zone.

Since N is large and the points are very close to each other, the quantity

$$\frac{1}{3N} \sum_{\mathbf{q},l} C(\nu, T)$$

may be replaced by

$$\int_0^{\nu_{\max}} C(\nu, T) g(\nu) d\nu,$$

where $g(\nu)d\nu$ is the fraction of the $3N$ frequencies that lie between ν and $\nu+d\nu$. The function $g(\nu)$ is known as the frequency distribution function. The problem of calculating the Debye-Waller factor and the total incoherent cross section therefore reduces to the calculation of this function.

B. Frequency Distribution Function

The method used to calculate $g(\nu)$ was to calculate $\nu_l(\mathbf{q})$ for a large number R of points equally spaced in the first Brillouin zone, and to count the number of times that a frequency between ν and $\nu+\Delta\nu$ occurred. This gives a good approximation for $g(\nu)$, provided R is large and $\Delta\nu$ is small. The computation was carried out by evaluating the function $F(\mathbf{q})$ for points whose coordinates were integral multiples of $b/30$. The number of points R was thus $60^3/2=108\,000$. The symmetry properties of Eq. (1) reduce the number of points for which the equation must be solved to 2792. The particular $g(\nu)$ function obtained from $F(\mathbf{q})$ is denoted by $G(\nu)$.

The maximum value of $F(\mathbf{q})$ is

$$\nu_{\max} = 8.96 \times 10^{12} \text{ sec}^{-1}.$$

For the calculation of $G(\nu)$, the frequency range was divided into intervals $\Delta\nu = 0.039 \times 10^{12} \text{ sec}^{-1}$. The curve obtained is shown in Fig. 11.

The function $g(\nu)$ is continuous, but its slope has a finite number of infinite discontinuities. Van Hove¹⁹

¹⁶ See Eq. (2.11) in reference 2. Note that the quantities \mathbf{q} , $\boldsymbol{\tau}$, $\boldsymbol{\kappa}$, and \mathbf{k} in reference 2 are 2π times the corresponding quantities in the present paper.

¹⁷ G. Placzek, Phys. Rev. **93**, 895 (1954).

¹⁸ Equation (8) is readily obtained from Eq. (4.4) in reference 2.

¹⁹ L. Van Hove, Phys. Rev. **89**, 1189 (1953).

has pointed out that the existence of such discontinuities is a direct consequence of the fact that the $\nu_i(\mathbf{q})$ function is periodic in the reciprocal lattice. This is because the discontinuities correspond to points in \mathbf{q} space where $\text{grad}_{\mathbf{q}} \nu_i = 0$, and the existence of such points is necessitated by the periodicity of the $\nu_i(\mathbf{q})$ function. The points are known as critical points and the corresponding frequencies, as critical frequencies.

The quantities $\alpha(T)$ and $\beta(T)$ were calculated without taking account of the critical frequencies. However, as a matter of interest, the critical points of the function $F(\mathbf{q})$ were investigated. Use was made of the fact, pointed out by Rosenstock,⁷ that the majority of the critical points lie in positions which are simply related to the symmetry planes and axes of the reciprocal lattice. All the critical points in the planes $q_3=0$ and $q_1=q_2$ were located, and the corresponding frequencies calculated. A search was made for further critical points, but none were found. It is thought that there are none for this particular $\nu_i(\mathbf{q})$ function.

The critical points of the function $F(\mathbf{q})$ are indicated in Fig. 2 by open circles. The points indicated by \diamond are examples of what Van Hove¹⁹ terms "generalized critical points." They can only occur at points where two of the frequencies are equal. Those that occur in the present instance do not give rise to any discontinuity in the slope of $g(\nu)$.

The shape of the $g(\nu)$ function near a critical frequency depends on the nature of the corresponding critical point, i.e., on whether it is a three-dimensional maximum (M), a three-dimensional minimum (m), a saddle point with a maximum in two dimensions and a minimum in the third (S_1), or a saddle point with a minimum in two dimensions and a maximum in the third (S_2).²⁰

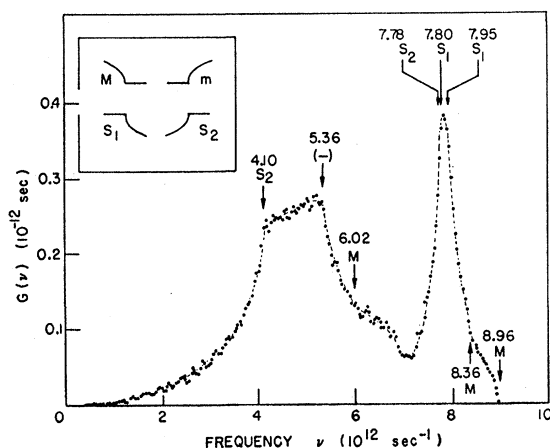


FIG. 11. Frequency distribution function $G(\nu)$ obtained from the function $F(\mathbf{q})$. The values and natures of the critical frequencies are shown. (The critical frequency $\nu = 5.36 \times 10^{12} \text{ sec}^{-1}$ is discussed in footnote 20.) The theoretical shape of the frequency distribution function near a critical frequency is indicated in the inset.

²⁰ These are the only types of critical points considered by Van Hove and Rosenstock, but other critical points may occur, at

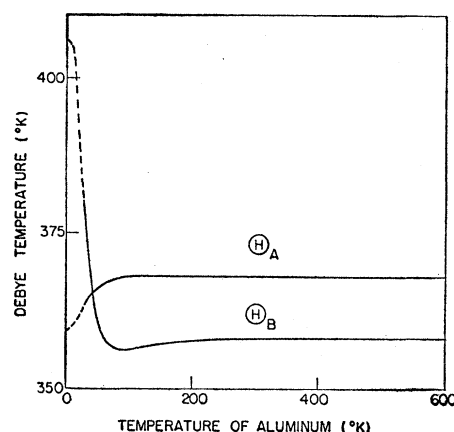


FIG. 12. Debye temperatures obtained from the frequency distribution function $G(\nu)$. The values between 0°K and 29°K were not calculated.

The values of the critical frequencies and the natures of the corresponding critical points are shown in Fig. 11. It can be seen that our approximation for the $g(\nu)$ function is sufficiently good to give the correct shape at some of the critical frequencies, e.g., $\nu = 4.10 \times 10^{12} \text{ sec}^{-1}$, but not at others.

C. Results and Discussion

The functions $\alpha(T)$ and $\beta(T)$ have been calculated at various temperatures. The results are given in terms of the Debye temperature Θ which, for a function $C(\nu)$ and a frequency distribution function $g(\nu)$, is defined by the relations

$$k_B \Theta = h \nu_D,$$

and

$$\frac{3}{\nu_D^3} \int_0^{\nu_D} C(\nu) \nu^2 d\nu = \int_0^{\nu_{\max}} C(\nu) g(\nu) d\nu.$$

The Debye temperatures for the Debye-Waller factor and for the cross section $\sigma^{(1)}$ for incident neutrons of long wavelength are denoted by Θ_A and Θ_B , respectively.

The values of Θ_A and Θ_B are plotted against temperature in Fig. 12. The figure shows that Θ_A is constant at temperatures above about 100°K , and Θ_B is constant at temperatures above about 200°K . However, it must be remembered that these results are based on the assumption that the forces are harmonic and, hence, that the vibration frequencies are independent of temperature. The effects of the anharmonic forces are such that the frequencies tend to decrease with tem-

least theoretically. An example of such a point occurs in the present case for the lowest frequency at the point 110 in reciprocal space, where the frequency has the value $5.36 \times 10^{12} \text{ sec}^{-1}$. This value is a maximum in the direction of the q_3 axis, but in the plane perpendicular to the q_3 axis, it is a minimum in the direction of the q_1 and q_2 axes and a maximum in the directions at 45 degrees to these axes.

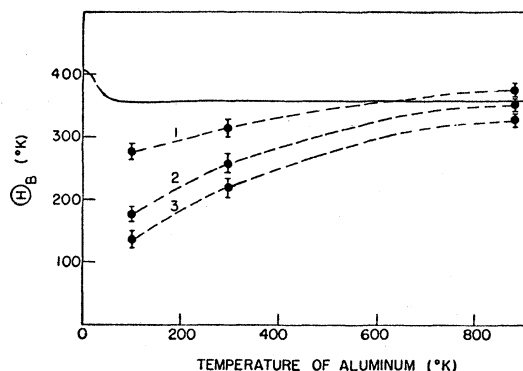


FIG. 13. Debye temperature for the total incoherent cross section for incident neutrons of long wavelength. The unbroken curve is the theoretical curve obtained from $G(\nu)$. The points are experimental values obtained from the results of Zimmerman and Palevsky²² on the assumption of the incoherent approximation. The values labeled 1, 2, and 3 are obtained from absorption cross sections of 0.135, 0.130, and 0.125 barns/A, respectively.

perature. It is therefore to be expected that at temperatures above about 200°K, Θ_A and Θ_B will in fact decrease with temperature.

Owen and Williams²¹ have obtained values for the Debye-Waller factor in aluminum by measuring the intensity of x-ray reflections as a function of T . At room temperature, they obtain a value of 395°K for Θ_A and find that, from $T=300^\circ\text{K}$ to $T=600^\circ\text{K}$, Θ_A decreases by 7°K per 100°K rise in T . Their room temperature value is somewhat higher than the value of 368°K obtained from our calculations. However, the uncertainty in the force constants used in the calculation of $G(\nu)$ results in an uncertainty in the calculated Debye temperature of about 20°K. When the error in the experimental value is taken into account, the two values are not inconsistent.

Experimental data for the quantity

$$\beta(T) \equiv \lim_{k_0 \rightarrow 0} k_0 \sigma^{(1)}$$

can only be obtained indirectly. Experimentally, the quantity measured is the sum of the total scattering and absorption cross sections. On the assumption of the incoherent approximation, viz, that the interference term² in the total scattering cross section is zero, the value of $\beta(T)$ may be obtained from measurements of the total cross section, together with a knowledge of

the absorption cross section. The results obtained from the measurements of Zimmerman and Palevsky²² are given in Fig. 13. The values obtained for Θ_B depend sensitively on the value adopted for the absorption cross section. The results have therefore been analyzed in terms of the accepted value of this cross section and also of the limiting values implied by its experimental uncertainty.

As can be seen from Fig. 13, the agreement between theory and experiment is rather poor at low temperatures. This is not due to the fact that the frequency distribution function used for calculating the theoretical values of Θ_B is based on room temperature force constants. The correction which must be made at low temperatures to take account of this causes Θ_B to increase, and the discrepancy is thereby increased.

If the experimental results and the assumed absorption cross section are correct, a possible explanation of the discrepancy is that the incoherent approximation does not apply to aluminum. To calculate the magnitude of the interference term, it is necessary to integrate an expression for the cross section over the scattering surfaces, a tedious task, which, in view of the present uncertainty of these surfaces, has not been undertaken.

ACKNOWLEDGMENTS

The function $F(\mathbf{q})$, the frequency distribution function $G(\nu)$, and the functions $\alpha(T)$ and $\beta(T)$ were computed on the Electronic Computer at the Institute for Advanced Study by Dr. H. Maehly, whom I wish to thank for his cooperation and efficiency. I am grateful to Dr. H. Goldstine for granting facilities on the Computer. The computation was supported by Army Contract No. DA-36-034-ORD-1646.

I wish to thank Professor R. Oppenheimer for his hospitality at the Institute, and the International Cooperation Administration of the U. S. Government for a Fellowship, during the tenure of which this work was done. I am grateful to Dr. C. Walker for making his results available to me in advance of publication and to Professor L. Van Hove and Dr. A. T. Stewart for their helpful comments on the manuscript.

I wish above all to record my indebtedness to the late Dr. G. Placzek for his suggestion of the problem and for his kind and valuable advice throughout the work.

²¹ E. A. Owen and R. W. Williams, Proc. Roy. Soc. (London) A188, 509 (1947).

²² R. L. Zimmerman and H. Palevsky, Phys. Rev. 98, 1162 (1955).